Numerical analysis of recovery stage with disappearing polymer layer RR-P3HT for the detection of DMMP based on diffusion equations

Tomasz Hejczyk, Jarosław Wrotniak, Paulina Powroźnik, and Wiesław Jakubik

Abstract—This document describes numerical analyses performed on a SAW gas sensor in a non-steady state. Our work involved predicting SAW velocity changes in relation to the surface electrical conductivity of the sensing layer. We found that the conductivity of the rough sensing layer (above a piezoelectric waveguide or quartz) is determined by the diffused gas molecule concentration profile inside it. Specifically, we present numerical results for the DMMP gas concentration profile (CAS Number 756-79-6) within an (RR)-P3HT layer during the non-steady state recovery step. The core of these investigations was to understand thin film interaction with target gases in a SAW sensor configuration, using the diffusion equation for polymers. The outcomes of these numerical analyses provide valuable insights for selecting sensor design conditions, including the sensor layer's morphology, thickness, operating temperature, and type. The numerical results, generated using Python code, are then elaborated upon and examined.

Keywords—gas sensors; numerical modeling; SAW gas Ingebrigtsen's formula: DMMP; acoustoelectric analysis (NAA)

INTRODUCTION

HE main goal of this research was to understand how thin films interact with target gases in a SAW sensor setup. We based our work on a simple reaction-diffusion equation [1], which is key to understanding things like heat or mass movement in porous materials. This paper brings together acoustoelectric theory (specifically Ingebrigtsen's formula) and looks at how gas diffusion concentration profiles change over time. It also predicts how a thin RR-P3HT layer [2] affects SAW wave velocity during recovery in an acoustic waveguide. When gas molecules diffuse into the sensor layer, their physical properties, especially electrical conductivity, change. This change then impacts the boundary conditions for wave propagation, leading to shifts in both wave attenuation and propagation velocity. SAW sensors can show two effects: electrical (acoustoelectric) and mass. Our paper focuses only on the electrical effect, as it's vital for sensors with a conductive layer. We showed how the DMMP

concentration profile behaves under conditions during recovery (see Fig. 1), presenting just the final equation that describes these time-dependent DMMP

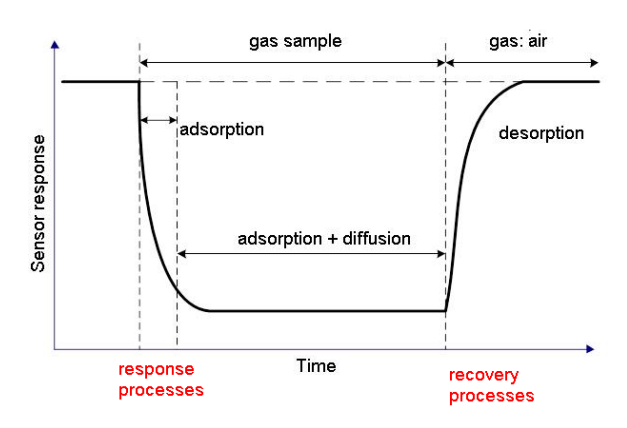


Fig. 1. Focusing on DMMP detection, this covers the gas diffusion dynamics occurring within a thin RR-P3HT layer gas sensor during its response and subsequent recovery steps

The primary goal of this investigation was to study the interaction of thin films with target gases in a SAW sensor configuration, based on a simple reaction-diffusion equation [1]. Diffusion equations offer the theoretical framework for analyzing physical phenomena such as heat or mass transport within porous or rough substrates. This paper summarizes the acoustoelectric theory, specifically Ingebrigtsen's formula, the dynamics of gas diffusion concentration profiles, and predicts the influence of a thin polymer sensor layer [27], [30] on SAW wave velocity in an acoustic waveguide (in this case, quartz [2]) during recovery steps [3]-[6].

Target gas molecules, like DMMP, diffuse from the outer surface into the porous or rough sensing layers. The diffusion of these gas molecules into the sensor layer alters its physical properties, particularly its electrical conductivity. This change in conductivity modifies the boundary conditions for wave propagation. Consequently, the attenuation of the SAW also changes its propagation velocity. In SAW sensors, both electrical (acoustoelectric) and mass effects can occur. This paper focuses exclusively on the electrical effect, which is significant in SAW sensors equipped with a conducting sensor layer. We analyzed the behavior of the DMMP gas



T. Hejczyk is with The Academy of Creative Development - the Foundation Marklowice, Poland (e-mail: t.hejczyk@ente.com.pl).

J. Wrotniak, P. Powroźnik and W. Jakubik are with Silesian University of Gliwice, Poland (e-mail: jaroslaw.wrotniak@polsl.pl, paulina.powroznik@polsl.pl, wjakubik@polsl.pl).

2 T. HEJCZYK, ET AL.

concentration profile [21] under non-steady-state conditions during recovery steps. The paper presents the final equation describing time-dependent concentration profiles using the recovery step method.

Changes in the electrical properties of sensor layers are dependent on the concentration of gas molecules in the volume, as well as the thickness, temperature, size of the gas molecules, layer morphology, and porosity of the sensing layer. We conducted a numerical analysis using a custom-developed Python program to evaluate the impact of these parameters on the sensor response during the recovery stage. The results obtained are crucial for the proper construction of a SAW sensor. This analysis is achievable by building upon a developed analytical model of a SAW sensor, supported by gas diffusion dynamics equations for thin film polymers [7].

SAW gas sensor model and the impact of gas diffusion on the acoustoelectric effect.

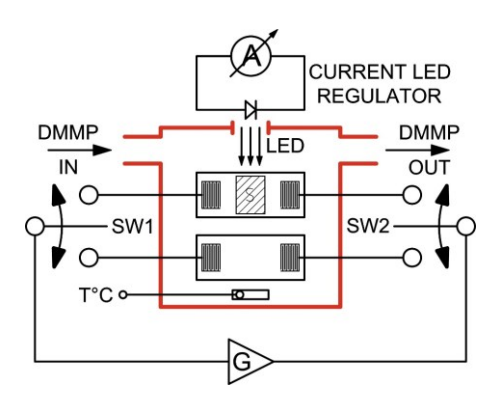


Fig. 2. Measuring system (incandescent lighting) - LED lighting [2], [8], [22]

The entry of gas particles into the sensor layer via diffusion leads to the formation of a distinct concentration distribution profile of these particles within the layer's depth. This gas diffusion phenomenon is fundamentally important for porous or rough layers that possess an extensive surface area. Such layers are deliberately created through specialized technological processes. It's noteworthy that high porosity or roughness directly contributes to a high sensitivity to gas exposure [4]-[6].

For optimal sensor design [20], developing an analytical model of the SAW sensor is essential. While initial models were stationary (steady-state), the inclusion of time dependencies has enabled dynamic characteristic studies of the SAW gas sensor [9]-[11].

In a SAW (Surface Acoustic Wave) sensor, the active polymer sensor layer is integrated onto a piezoelectric waveguide, which serves as the core measuring system (Fig. 2). In these sensors, the surrounding gas significantly affects the electrical conductivity (known as the acoustoelectric phenomenon) of the sensor layer. This effect becomes particularly pronounced when the layer exhibits porosity or roughness. Knudsen diffusion [3]-[6], [9]-[11] can play a vital role, especially since pore diameters typically range from 1-2 nm to 100 nm in radius [19], [24]. This type of diffusion is particularly crucial for sensor applications. The profiles of concentration are influenced by the gas molecules present in

the sensor layer, as well as the ratio between the constant reaction rate (k_D) and the diffusion coefficient (D_K) . As a kinetic phenomenon, diffusion is time-dependent. Consequently, the distribution profile of gas molecules within the layer changes with the passage of time, both during the initial response and the subsequent recovery steps. Analyzing this time-dependent phenomenon enables the evaluation of the sensor's regeneration capability over time.

The concentration of gas molecules within the layer is mathematically expressed as a function of time (t) and depth (y) within this resistive layer. The methodology employing Fourier transforms, as presented by N. Matsunagi, G. Sakai, K. Shimanoe, and N. Yamazone [1], has been utilized. Specifically, the concentration C(y,t) during the recovery step can be described by equations 1, 2, 3, and 4 [1], [12], [16].

$$\frac{\delta C(x,t)}{\delta t} = D \frac{\delta C^{2}(x,t)}{\delta x^{2}} - kC(x,t) - Bs \frac{\delta C(x,t)}{\delta x}$$

$$\begin{cases} \frac{\partial C_{A}(x,t)}{\partial t} = D \frac{\partial^{2} C_{A}(x,t)}{\partial x^{2}} - kC_{A}(x,t) \\ \frac{\partial C_{A}(x,t)}{\partial t} = D \frac{\partial^{2} C_{A}(x,t)}{\partial x^{2}} - Bs \frac{\partial C_{A}(x,t)}{\partial x} \end{cases}$$

$$C_{A}(x,t) = v(x,t) + w(x,t) + z(x,t)$$

$$(3)$$

$$C_{A}(x,t) = \frac{c_{S}\sqrt{D}}{L} \sum_{n=1}^{\infty} \frac{exp(-\omega_{n}^{2}t) \cdot [1-(-1)^{n}]}{\omega_{n}} \cdot sin \frac{n\pi}{2L} x = 4 \cdot C_{A,S} \sum_{n=1}^{\infty} \frac{[1-(-1)^{n}]}{2} exp(-\omega_{n}^{2}t) \frac{1}{n\pi} sin \frac{n\pi}{2L} x$$
(4)

where $\omega_n = \frac{n\pi\sqrt{D_K}}{2L}$, these terms refer to: the

concentration $C_{A,S}$ at the top surface of the sensor layer; n, which denotes the number of iterations; and L, representing the thickness of the semiconducting sensor layer.

To resolve formula eq. 1 we must have solution of the homogeneous differential equation (5) - 1 step.

$$\frac{\partial v(x,t)}{\partial t} = D \frac{\partial^2 v(x,t)}{\partial x^2}$$

$$v(x,t) = \sum_{n=1}^{\infty} T_n(t) \sin \frac{n\pi}{2L} x,$$
(6)

Where

$$T_n(t) = \exp(-\omega_n^2 t)c_n,$$

Fig. 3 Equivalent model on recovery step

Identical film

$$\begin{aligned} c_n &= T_n(0) = \frac{2}{2L} \int_0^{2L} v(x,0) \sin \frac{n\pi}{2L} x dx \\ c_n &= T_n(0) \\ &= \frac{2}{2L} C_{A,S} G_k \frac{(2m-1)\pi}{L} \left[\left(\frac{exp\left(\frac{b_1}{2}x - \frac{\sqrt{4k_1 + b_1^2}}{2}x\right)}{\left(\frac{b_1}{2} - \frac{\sqrt{4k_1 + b_1^2}}{2}\right)^2 + \left(\frac{n\pi}{2L}\right)^2} \right) \\ &- \left(\frac{exp\left(\frac{\sqrt{4k_1 + b_1^2}}{2}x + \frac{b_1}{2}x\right)}{\left(\frac{\sqrt{4k_1 + b_1^2}}{2} + \frac{b_1}{2}\right) + \left(\frac{n\pi}{2L}\right)^2} \right) \right] \end{aligned}$$

 $v(x,t) = \sum exp(-\omega_m^2 t)$ $\left\{ C_{A,s} G_k \frac{(2m-1)\pi}{L^2} \left| \left(\frac{exp\left(\frac{b_1}{2}x - \frac{\sqrt{4k_1 + b_1^2}}{2}x\right)}{\left(\frac{b_1}{2} - \frac{\sqrt{4k_1 + b_1^2}}{2}\right)^2 + \left(\frac{n\pi}{2L}\right)^2} \right) \right| \right\}$ $-\left(\frac{exp\left(\frac{\sqrt{4k_{1}+b_{1}^{2}}}{2}x+\frac{b_{1}}{2}x\right)}{\left(\frac{\sqrt{4k_{1}+b_{1}^{2}}}{2}+\frac{b_{1}}{2}\right)+\left(\frac{n\pi}{2}\right)^{2}}\right)\right|$ $\cdot \sin \frac{(2m-1)\pi}{2I}x$

 $+4 \cdot C_{A,s} \sum_{n=1}^{\infty} exp(-\omega_n^2 t) \frac{1}{n\pi} sin \frac{n\pi}{2I} x$

where n = 2m-1

2 step – solvation non-homogeneous differential equation:

$$\frac{\partial w(x,t)}{\partial t} = D \frac{\partial^2 w(x,t)}{\partial x^2} + f(x,t)$$
(9)

Assuming that:

(7)

$$w(x,t) = \sum_{n=1}^{\infty} T_n(t) \sin \frac{n\pi}{2L} x$$
(10)

$$f(x,t) = \sum_{n=1}^{\infty} f_n(t) \sin \frac{n\pi}{2L} x$$

(11)

3

$$w(x,t) = -\frac{k}{L} \sum_{n=1}^{\infty} A_n \sin \frac{n\pi}{2L} x$$

$$A_n = \int_0^t \int_0^{2L} \exp\{(-\omega_n^2(t-\tau))\}C(x,\tau)\sin \frac{n\pi}{2L} x dx d\tau$$
(13)

3 step - solvation non-homogeneous differential equation

$$z(x,t) = \sum_{n=1}^{\infty} T_n(t) \sin \frac{n\pi}{2L} x$$

$$z(x,t) = -\frac{Bs}{L} \sum_{n=1}^{\infty} A_n \sin \frac{n\pi}{2L} x$$

$$(15)$$

$$\frac{dC(x,\tau)}{dx} = -\frac{Bs}{L} \sum_{n=1}^{\infty} \left(\frac{n\pi}{2L}\right)^{2} (-1) A_{n} \sin \frac{n\pi}{2L} x \cdot C_{A,s}$$
(16)

$$A_{n} = \int_{0}^{t} \int_{0}^{2L} exp[(-\omega_{n}^{2}(t-\tau)] \frac{dC(x,\tau)}{dx} cos(\frac{n\pi}{2L}x) dxd\tau$$
(17)

Solution of the differential equation of the diffusion in nonsteady state on recovery step. Solution C(x,t):

$$C(x,t) = v(x,t) - \frac{k}{L} \sum_{n=1}^{\infty} A_n \sin \frac{n\pi}{2L} x - \frac{Bs}{L} \sum_{n=1}^{\infty} A_n \sin \frac{n\pi}{2L} x$$
(18)

Numerical analysis in python gives solution

T. HEJCZYK, ET AL.

$$v(x,t) = \sum_{m=1}^{\infty} exp(-\omega_{m}^{2}t)$$

$$\begin{cases} C_{A,s}G_{k} \frac{(2m-1)\pi}{L^{2}} \left[\frac{exp\left(\frac{b_{1}}{2}x - \frac{\sqrt{4k_{1} + b_{1}^{2}}}{2}x\right)}{\left(\frac{b_{1}}{2} - \frac{\sqrt{4k_{1} + b_{1}^{2}}}{2}\right)^{2} + \left(\frac{n\pi}{2L}\right)^{2}} \right] \\ - \left(\frac{exp\left(\frac{\sqrt{4k_{1} + b_{1}^{2}}}{2}x + \frac{b_{1}}{2}x\right)}{\left(\frac{\sqrt{4k_{1} + b_{1}^{2}}}{2} + \frac{b_{1}}{2}\right) + \left(\frac{n\pi}{2L}\right)^{2}} \right) \\ \cdot sin\frac{(2m-1)\pi}{2L} + C_{A,s}\sum_{n=1}^{\infty} exp(-\omega_{n}^{2}t) \frac{1}{n\pi} sin\frac{n\pi}{2L}x \end{cases}$$
(19)

where n = 2m-1 and first, second term vanishes, third term is non zero.

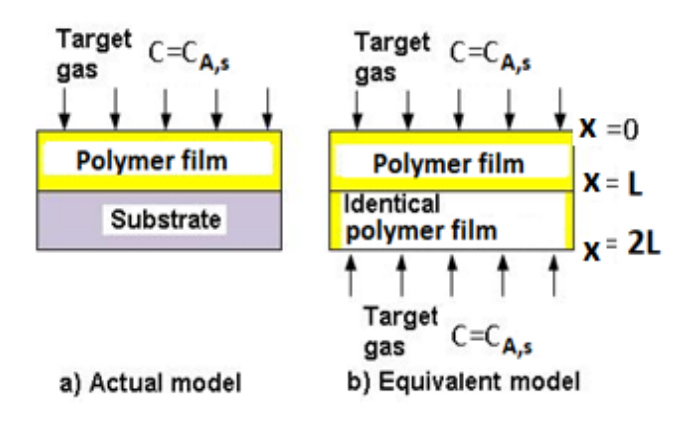


Fig. 4. We present the actual (a) and equivalent (b) models that are relevant during the recovery step [1],[12].

In the event that the target gas is suddenly switched off (Fig. 1), the system's initial state is defined by a concentration $C_A(x,0)$, along with the boundary conditions $C_A(0,t)=C_{A,S}$ and $C_A(2L,t)=0$ [1],[12]. The aforementioned formula provides the means to analyze the evolving concentration-time profile of gas molecule distribution.

A steady-state numerical analysis (NNA) of the acoustoelectric interaction in the sensing layer

Acousto-electric effect [23], [29] depends from the profile distribution in the layer, ie. from the distance particles of gas from surface acoustic waveguide.

To determine response sensor common impedance was designated. By incorporating impedance, which holds data on the gas molecule concentration profile in the layer, into the Ingebrigtsen formula [14, 15], we can effectively describe the relative change in surface acoustic wave (SAW) velocity in both steady-state and transient modes. The analytical expressions lucidly define the SAW sensor model (Fig. 5).

This model then formed the foundation for numerical analyses of the sensor's response. The findings from these numerical analyses are presented in the following section.

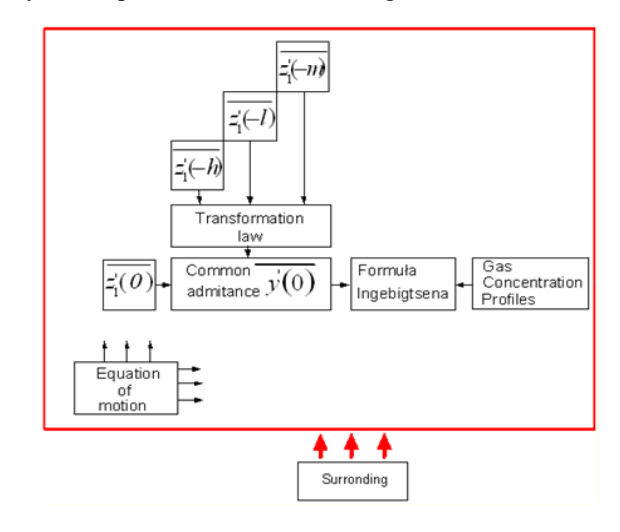


Fig. 5. Schematic diagram of the SAW sensor model

To conduct a numerical analysis of the SAW gas sensor, we utilized its established analytical model [25, 26]. For the sensor's layer, we made two key assumptions: first, that it consists of a uniform stack of infinitesimally thin sheets with a variable concentration of gas molecules (Fig. 5); and second, that this variable concentration impacts the electric conductance [10].

$$\frac{\Delta v}{v_0} = -Re\left\{\frac{\Delta k}{k_0}\right\} = -\frac{K^2}{2}$$

$$\cdot \left[\sigma_{T_2}(1 + aC_{A,y=0}) + \sum_{i=1}^{n-1} \sigma_{T_2}(y_i) f(y_i, \sigma_{T_2}(y_i))\right]^2,$$

vhere

$$ZZ = \left[\sigma_{T_2}(1 + aC_{A,y=0}) + \sum_{i=1}^{n-1} \sigma_{T_2}(y_i) f(y_i, \sigma_{T_2}(y_i))\right]^2 + \left[1 + \sum_{i=1}^{n-1} g(y_i, \sigma_{T_2}(y_i))\right]^2 (v_0 C_S)^2,$$
(20)

where: n – number of sublayers and $C_S = \varepsilon_0 + \varepsilon_p^T$,

$$\sigma_{T_2} = \sigma_{T_1} \exp\left(\frac{E_g}{2k_B} \cdot \frac{T_2 - T_1}{T_1 T_2}\right)$$
 $T_1 = 300 \text{K}, \quad \sigma_{T_1} = \sigma_0$

 $k_{\rm B}$ – Boltzman constant, $E_{\rm g}$ – band gap energy, \mathcal{E}_0 and $\varepsilon_{\rm p}^T$ are respectively, denoted are the dielectric permittivity of the vacuum and the piezoelectric substrate, respectively; the superscript T signifies a constant stress condition. Functions f(21) and g(22) in expression (20) are obtained by transforming the individual sublayers on the surface of the sensor waveguide (Fig. 15), and their form is given by:

$$f(y_i, \sigma(y_i)) = \frac{1 - \left[\operatorname{tgh}(ky_i) \right]^2}{\left[1 + \operatorname{tgh}(ky_i) \right]^2 + \left[\operatorname{tgh}(ky_i) \cdot \frac{\sigma(y_i)}{\varepsilon_0 v_0} \right]^2}$$
(21)

$$g(y_{i}, \sigma(y_{i})) = \frac{\left[1 + \operatorname{tgh}(ky_{i})\right]^{2} + \operatorname{tgh}(ky_{i}) \cdot \left(\frac{\sigma(y_{i})}{\varepsilon_{0}v_{0}}\right)^{2}}{\left[1 + \operatorname{tgh}(ky_{i})\right]^{2} + \left[\operatorname{tgh}(ky_{i}) \cdot \frac{\sigma(y_{i})}{\varepsilon_{0}v_{0}}\right]^{2}}$$
(22)

Utilizing this solution within the analytical model of the SAW sensor [4]-[7], [9]-[11], [17] enables the analysis of its dynamic recovery response. The temporal and spatial distribution of gas molecules in the sensor layer is governed by parameters including the reaction rate (here, photodegradation, k_D), the diffusion constant (D_K) , time, and temperature. The precision of numerical calculations directly correlates with the number of iterations (n), highlighting the clear dependence of concentration profiles on diffusion parameters. Our results, derived using various diffusion constants (D_K), demonstrate convergence when compared with studies by Matsunaga and Sakai and others [1], [12]. Figure 4 illustrates the gas profile under specific conditions: n=10 iterations, t=10 ms,1 s,10 s, reaction rates $k_D=10^8 s^{-1}$ and $B=10^5 s^{-1}$, and a Knudsen's diffusion constant D_K=10¹² nm²s⁻¹. We found that increasing iterations enhances method accuracy. Our analysis, consistent with [1], [12], further indicates that non-stationary state analysis during recovery time is critically important for the time range of $t=10^{-2}$ to 10 seconds (Fig. 6).

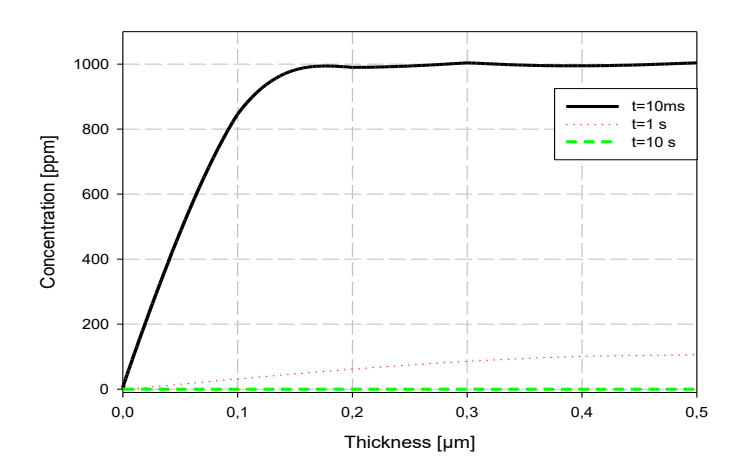


Fig. 6. Gas concentration profiles as a function of terations n=10, at Cs=1000 ppm, t=10 ms, 1s, 10s, k_D =10⁸ s⁻¹, Bs= υ = 10⁵ ms⁻¹ [13], D_K =10¹² nm²s⁻¹

Analyzing the acoustoelectric interaction in the sensing layer numerically during the recovery phase

This problem was numerically analyzed by assuming a constant concentration of gas molecules at the sensor layer's surface and in its surroundings. Relative wave velocity changes were determined numerically, taking into account the gas molecule concentration on the surface ($C_{A,S}$), mean roughness, layer thickness (L), and temperature (T) [28]. We performed a non-steady state analysis, varying time from 10^{-6} sec to 10^{-12} sec. This was predicated on the assumption that the gas molecule concentration profile in the sensor layer reaches steady state after 10-6 sec. The recovery state analysis, presented in Figures 7-10, allows for observation of

temporal changes in the sensor's response. The response of the polymer (RR)-P3HT to DMMP during recovery was examined based on gas concentration (Fig. 7), roughness (Fig. 8), layer thickness (Fig. 9), and temperature [18] (Fig. 10).

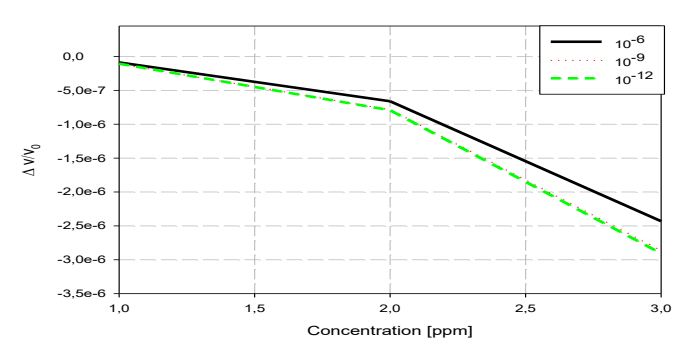


Fig. 7. Relative changes of velocity vs. concetration of the layer (RR)-P3HT in the time t=10⁻¹², 10⁻⁹, 10⁻⁶ s at n=2, a=-14,5, $D_{\rm K}$ = 10⁶ μ m²/s, $\sigma_{\rm s}$ =5 x 10⁻⁴, B=10³, s=10², Bs=0= 10⁵ ms⁻¹ [13], L=500nm, Gas: DMMP, T=300.0K Recovery step $E_{\rm g}$ = 2 eV, M=124,08 g/mol, K²/2(quartz) =0,09%

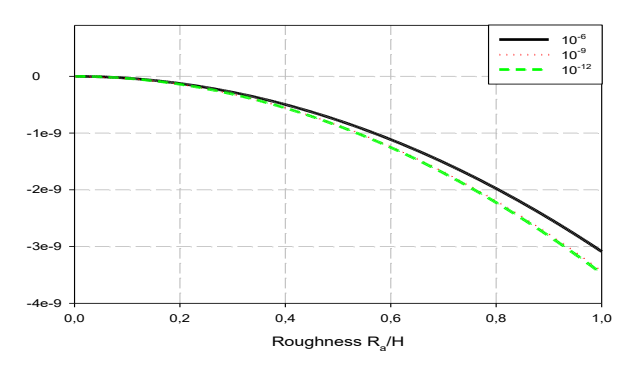


Fig. 8. Relative changes of velocity vs. roughness of the layer (RR)-P3HT in the time t=10⁻¹² , 10⁻⁹, 10⁻⁶ s at n=2, a=1, $D_{\rm K}$ = 10⁶ μ m² /s, $\sigma_{\rm s}$ =5 x 10⁻⁴, B=10³, s=10², Bs= υ = 10⁵ ms⁻¹ [13], L=500nm. Gas: DMMP, T=300K, concentration 2 ppm, $E_{\rm g}$ = 2 eV, M=124,08 g/mol, K2/2 (quartz) =0,09%

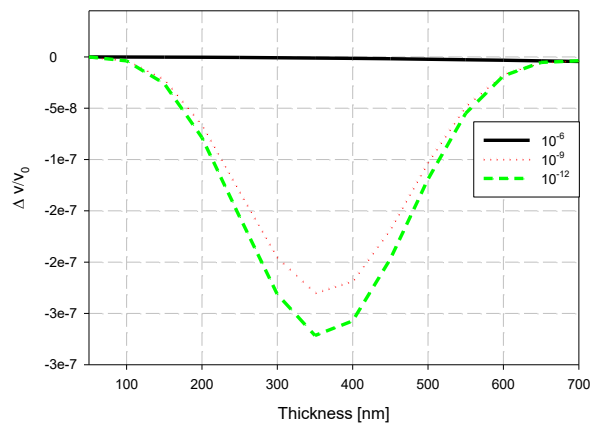


Fig. 9. Relative changes of velocity vs. thickness of the layer (RR)-P3HT in the time t=10⁻¹², 10⁻⁹, 10⁻⁶ s at n=2, a= -14,5, $D_{\rm K}$ = 10⁶ μ m²/s, σ _s=5 x 10⁻⁴, B=10³, s=10², Bs= υ = 10⁵ ms⁻¹ [13], Gas: DMMP, T=300K, concentration 2 ppm, multiplier 25, $E_{\rm g}$ = 2,7 eV, M=124,08 g/mol, K²/2 (quartz) =0,09%

6 T. HEJCZYK, ET AL.

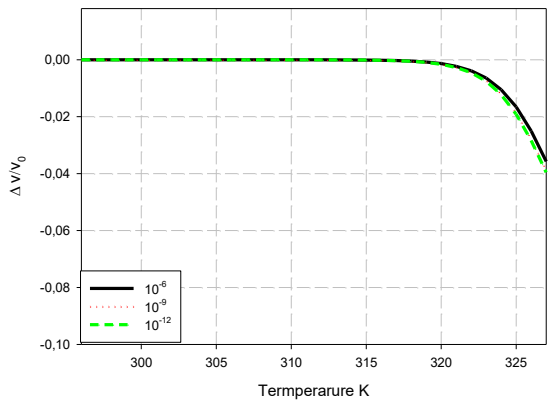


Fig. 10. Relative changes of velocity vs. temperature of the layer (RR)-P3HT in the time t=10⁻¹², 10⁻⁹, 10⁻⁶ s at n=2, a=5, $D_{\rm K}$ = 10⁶ μ m² /s, $\sigma_{\rm s}$ =5 x 10⁻⁴, B=10³, s=10², B= υ = 10⁵ ms¹ [13], L=500nm. Gas: DMMP, concentration 2 ppm, $E_{\rm g}$ = 2,7 eV, M=124,08 g/mol, K²/2 (quartz) =0,09%

Results from Experiments

The sensor's response fundamentally depends on adsorption, diffusion, and desorption processes. These processes are significantly impacted by temperature, gas molecule concentration, and the inherent properties of the sensor layer, including its thickness and roughness. In practical applications, measurements are normalized to facilitate comparison between different sensors. The time-dependent response characteristics provide crucial information about the sensor layer's properties, allowing for validation of its assumed parameters. Experimental response characteristics are detailed in Figures 11-12. Our analysis indicates that processes within the sensor layer are remarkably swift, occurring within microseconds. Consequently, findings from theoretical analysis are vital for examining and validating the sensor's dynamic response. Figure 1 presents the time characteristics, incorporating the inertia of the measuring chamber. For the given DMMP concentration, the estimated response time is 10-20 seconds, and the regeneration time is 7 minutes.

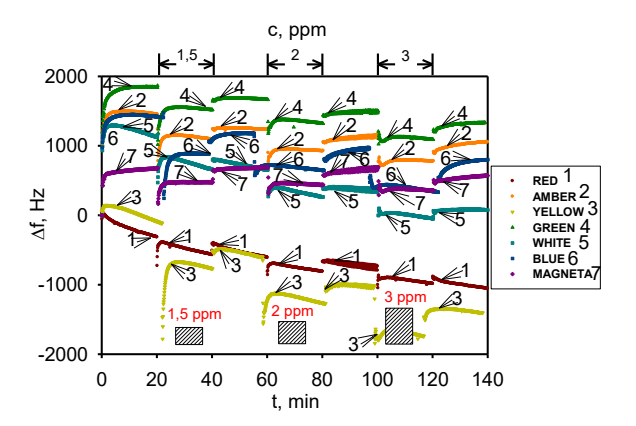


Fig. 11 For this experiment, we utilized a (RR)-P3HT sensor layer (500 nm thick) and exposed it to DMMP gas at concentrations of 1.5, 2, and 3 ppm. Illumination was provided by a 200 mA diode operating at selected wavelengths. The output recorded was the relative change in velocity plotted against time (and concentration) [2, 7]

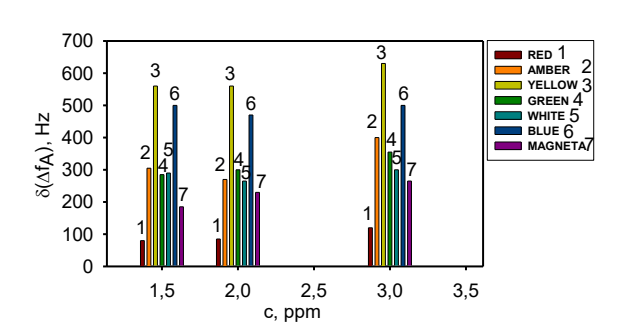


Fig. 12 Our experiment utilized a (RR)-P3HT sensor layer (500 nm thick) and exposed it to DMMP gas at 1.5, 2, and 3 ppm. A 200 mA diode (selected wavelengths) provided illumination. The resulting data includes a histography and measurements of the relative change of velocity against time (concentration)

CONCLUSION

The recovery state is clearly visible within the time range of 10^{-12} to 10^{-6} seconds. Our analyses indicated that the steady state of the sensor's responses is achieved after a few microseconds. This time depends on sensor layer parameters such as: photodegradation parameter (k), B, special polymer parameter (s) [13], diffusion constant (D_K), temperature (T), thickness (L), gas concentration (C_{A,S}), and the type of gas.

Both theoretical and experimental studies have confirmed the usefulness of the analytical model for designing SAW sensor parameters. The theoretical results for a selected layered sensing structure were experimentally verified and confirmed.

ACKNOWLEDGEMENTS

The Foundation ARK partially financed this work using its own funds. The corresponding author is grateful to Prof. Wiesław Jakubik, Dr. Jarosław Wrotniak, and Dr. Paulina Powroźnik for facilitating involvement in gas sensor development and for permitting the use of their research outcomes

REFERENCES

- N. Matsunga, G. Sakai, K. Shimanoe, N. Yamazoe, "Formulation of gas diffusion dynamics for thin film semiconductor gas sensor based on simple reaction-diffusion equation", Sensors and Actuators B, 96, pp. 226-233,2003
- [2] J. Wrotniak, W. Jakubik, P. Powroźnik, A. Stolarczyk, M. Magnuski, Acoustic tests of RR- P3HT type polymer for the detection of DMMP in the air [in Polish: Akustyczne badania polimeru typu RR-P3HT do wykrywania DMMP w powietrzu, Przegląd Elektrotechniczny, 94(6): 70-73, 2018 https://doi.org/10.15199/48.2018.06.12
- [3] T. Hejczyk, M. Urbańczyk, "WO₃-Pd Structure in SAW Sensor Hydrogen Detection", Acta Physica Polonica A, 120, 4, 616-620, 2011
- [4] T. Hejczyk, M. Urbańczyk, W. Jakubik, "Analytical Model of Semiconductor Sensor Layers in SAW Gas Sensors", Acta Physica Polonica A, 118, 6, 1148-1152, 2010.
- [5] T. Hejczyk, M. Urbańczyk, T. Pustelny, W. Jakubik, "Numerical and Experimental Analysis of the Response of a SAW Structure with WO₃ layers an Action of Carbon Monoxide", Archives of Acoustics 40, 1, 19-24, 2015.
- [6] T. Hejczyk, M. Urbańczyk, R. Wituła, E. Maciak, "SAW sensors for detection of hydrocarbons. Numerical analysis and experimental results", Bulletin of the Polish Academy of Sciences: Technical Sciences, 60, 3, 589-595, 2012.

- [7] T. Hejczyk, J. Wrotniak, M. Magnuski, W Jakubik. Experimental and Numerical Acoustoelectric Investigation of the New SAW Structure with (RR)-P3HT Polymer in DMMP Detection, Archives of Acoustics, Vol. 46, No. 2; p. 313–322, 2021, https://doi.org/10.24425/aoa.2021.136585.
- [8] M. Magnuski, J. Wrotniak J, Patent no PAT.230526,"System for detecting chemical compounds in gaseous atmospheres, with a sensor using surface acoustic waves (SAW)", 2016.
- [9] M. Urbańczyk, "Analytical model of a SAW gas sensor", WIT Transactions on Computational Methods and Experimental Measurements, Proceedings of the CMEM11, WIT Press Southampton, 48, 229-239, 2011.
- [10] M. Urbańczyk, "Gas Sensors on the base of Surface Acoustic Wave. 2011 Monograph, Edited by SUT, Gliwice, 2013 (in Polish).
- [11] M. Urbańczyk, T.Hejczyk, "Analysis of non-steady state in SAW gas sensors with semiconducting sensor layers", Acta Physica Polonica A, 120, 4, 789-793,2011.
- [12] N. Matsunga, G. Sakai, K. Shimanoe, N. Yamazoe, (2001), "Diffusion equation-based study of thin film semiconductor gas sensor-response transient", Sensors and Actuators B, 83, 216-221, 2001.
- [13] J. Crank, "The Mathematics of Diffusion", formula in page. 262, OxfordUniversity Press, 1975.
- [14] B.A. Auld Acoustic Fields and Waves, 2, Wiley, New York; p. 271-290, 1973.
- [15] T. Hejczyk, T. Pustelny Analysis of the Saw System with the PANI + Nafion Sensing Structure for Detection of Low Concentration Carbon Monoxide, Archives of Acoustics, Vol. 45, No. 4; pp. 681–686, 2020 https://doi.org/10.24425/aoa.2020.135274.
- [16] T. Hejczyk, J. Wrotniak, P. Powroźnik, W. Jakubik, "Numerical analysis and new formulas of the response stage, on recovery step, of a new SAW Structure with disappeared layer RR-P3HT in detection DMMP", WSW&QA, 2025, https://doi.org/10.5162/20WWonAE/A9.
- [17] T. Hejczyk, T. Pustelny, B. Wszołek, W. Jakubik Numerical Analysis of Sensitivity of SAW Structure to the Effect of Toxic Gases, Archives of Acoustics 41, 4; p. 747–755, 2016, https://doi.org/10.1515/aoa-2016-0072
- [18] P. Sakiewicz, R. Nowosielski, R. Babilas, D. Gasiorek D, M. Pawlak, FEM simulation of Ductility Minimum Temperature (DMT) phenomenon in CuNi25 alloy, Journal of Achievements in Materials and Manufacturing Engineering, 61, issue 2, Dec. p. 274-280, 2013.
- [19] A. Michalska, A. Polyaniline micro- and nanostructures for biomedical applications, PhD Thesis (in Polish), 2011.

- [20] T. Hejczyk, G. Kamiński, R. Ogaza, Patent no PL 229696 B1, Application of the hybrid sensor with acoustic surface wave [in Polish]. p. 2-5, 2018.
- [21] P. Powroźnik, W. Jakubik, A. Kaźmierczak-Bałata, Detection oforganophosphorus (DMMP) vapour using phthalocyanine-palladium bilayer structures, EUROSENSORS, Procedia Engineering, 120; P. 368 – 371, 2015, https://doi.org/10.1016/j.proeng.2015.08.640.
- [22] K. Jasek, W. Miluski, M. Pasternak, New approach to saw gas sensors array response measurement, Acta Physica Polonica A, 120(4), p. 639– 641, 2011, https://doi.org/10.12693/APhysPolA.120.639.
- [23] B. Pustelny, T. Pustelny, Transverse acoustoelectric effect applying in surface study of GaP: Te(111), Acta Physica Polonica A, 116, 3; p. 383 384, 2009, https://doi.org/10.12693/APhysPolA.116.383.
- [24] T. Pustelny, M. Procek, E. Maciak, A. Stolarczyk, S. Drewniak, M. Urbanczyk, M. Setkiewicz, K. Gut, Z. Opilski, Gas sensors based on nanostructuures of semiconductor ZnO and TiO2, Bulletin of the Polish Academy of Sciences: Technical Sciences, 60, 4; p. 853–859, 2012.
- [25] A. Kawalec, M. Pasternak, Microwave humidity sensor based on surface acoustic wave resonator with nafion layer, IEEE Transactions on Instrumentation and Measurement, 9(57); p. 2019–2023, 2008.
- [26] A. Kawalec, M. Pasternak M, K. Jasek, Measurements results of SAW humidity sensor with nafion layer, European Physical Journal: Special Topics, 154; P. 121–126, 2008.
- [27] R. Yoo, J. Kim, M. J. Song, W. Lee, J. S. Noh, Nano-composite sensors composed of single-walled carbon nanotubes and polyaniline for the detection of a nerve agent simulant gas, Sensor. Actuat. B-Chem, 209; 2015. p. 444-448, https://doi.org/10.1016/j.snb.2014.11.137.
- [28] T. Hejczyk, M. Urbańczyk, Numerical Optimization of Structures SAW Gas Sensors, Acta Physica Polonica A Vol. 124 No. 3.; p.432-435, 2013, https://doi.org/10.12693/APhysPolA.124.432.
- [29] T. Pustelny, A. Opilski, B. Pusteny, Determination of some kinetic parameters of fast surface states in silicon single crystals by means of surface acoustic wave method Acta Physica Polonica A Volume 114, Issue 6 A, p. A183-A190, 2008.
- [30] Y. Long, Y. Wang, X. Du, L. Cheng, P. Wu, Y. Jiang, The different sensitive behaviors of a hydrogen-bond acidic polymer-coated SAW sensor for chemical warfare agents and their simulants, Sensors, 15; p. 18302–18314, 2015, https://doi.org/10.3390/s150818302.